Selected-Control Synthesis of NaV 6 O 15 and Na 2 V 6 O 16 ·3H 2 O Single-Crystalline Nanowires

ARTICLE *in* CRYSTAL GROWTH & DESIGN · MAY 2005

Impact Factor: 4.89 · DOI: 10.1021/cg0496686

3 AUTHORS, INCLUDING:

Gen-Tao Zhou
University of Science and Technology of China
60 PUBLICATIONS **775** CITATIONS

CRYSTAL GROWTH & DESIGN
2005
VOL. 5, NO. 3
969−974

Selected-Control Synthesis of NaV_6O_{15} and $Na_2V_6O_{16}\cdot 3H_2O$ Single-Crystalline Nanowires

Gen-Tao Zhou,*,† Xinchen Wang,‡ and Jimmy C. Yu*,‡

School of Earth and Space Sciences, University of Science and Technology of China, Hefei 230026, P. R. China, and Department of Chemistry, The Chinese University of Hong Kong, Shatin, New Territories, Hong Kong

Received October 1, 2004

ABSTRACT: NaV_6O_{15} and $Na_2V_6O_{16}\cdot 3H_2O$ nanowires were selectively prepared from the reaction between V_2O_5 and $NaHSO_4\cdot H_2O/Na_2SO_4$ under hydrothermal conditions. The synthesized products were characterized by XRD, SEM, TEM, SAED, EDX, HRTEM, and XPS analytical techniques. SAED and HRTEM analyses confirm the single-crystalline nature of both NaV_6O_{15} and $Na_2V_6O_{16}\cdot 3H_2O$ nanowires. The nanowires of NaV_6O_{15} are uniform and straight, with around 80 nm in diameter and several tens of micrometers in length. $Na_2V_6O_{16}\cdot 3H_2O$ nanowires have an average diameter of 60 nm and length up to 10 μm. The key factors to control the phase composition and morphology, such as the amount of sulfates and the selective absorption of SO_4^{2-} in different crystal facets, are discussed. The optimum hydrothermal temperatures for the nanowire growth are 180 °C for NaV_6O_{15} and 180 to 140 °C for $Na_2V_6O_{16}\cdot 3H_2O$. A tentative formation mechanism is proposed.

Introduction

One-dimensional (1D) nanostructures, such as nanorods, nanowires, and nanotubes, have attracted extensive attention as a result of their novel size- and morphology-dependent properties. These 1D nanostructured materials have exhibited novel optical, electrical, magnetic, and mechanical properties that are very different from that of bulk or nanoparticle materials.[1] It has also been noted that some 1D nanostructured materials have been used as active components or interconnects in fabricating nanoscale electronic, optical, optoelectronic, electrochemical, and electromechanical devices. Outstanding samples include field-effect transistors (FETs),[2] light-emitting diodes (LEDs),[3] single-electron transistors,[4] biological and chemical sensors,[5] photodetectors,[6] electron emitters,[7] and ultraviolet lasers.[8]

The key to preparing a 1D nanostructure is the way in which atoms or other building blocks are rationally assembled into a structure with nanometer size but a much larger length.[9a] Strategies for the preparation of 1D nanowires include formation from a confided alloy droplet, as described by the vapor−liquid−solid (VLS) growth mechanism [9] and an analogous solution−liquid−solid (SLS) growth process.[10] Other methods have also been reported including oxide-assisted growth (OAG),[11] physical evaporating[1c,d] and CVD methods,[12] the kinetic control of growth through the use of capping reagents, and the use of template-inspired methodologies.[13] Many of these have been reviewed recently by Rao et al.[14] and Xia et al.[15] Although these strategies have been developed for the synthesis of nanowires, they typically suffer from the requirements of high temperature, special conditions, tedious procedures, and catalysts or templates. In particular, the introduction of templates or catalysts to the reaction system tends to make the synthetic process much more complicated, and may bring about an increase of impurity concentration in the final product. Therefore, a simple and effective methodology for the synthesis of 1D nanowires would be much preferred by nanoscience researchers. Recently, low-temperature solution-phase synthesis has been proposed as an attractive approach toward 1D nanosized materials of high crystallinity.[15,16]

The utilization of vanadium pentoxide-based compounds is a subject of intensive studies. The unique physical−chemical properties of these compounds allow a wide range of practical applications such as electrochromic devices, cathodic electrodes for lithium batteries, humidity sensors, and so on.[17] The interest in NaV_6O_{15} ($Na_{0.33}V_2O_5$) was strongly increased owing to the charge ordering and magnetic ordering occurring in this compound with mixed-valence states $V^{5+}(3d^0)$ and $V^{4+}(3d^1)$.[18] These compounds are usually prepared by means of high-temperature solid-state reactions. Recently, $CaV_6O_{16}\cdot 3H_2O$ and $Na_2V_6O_{16}\cdot 3H_2O$ nanobelts have been synthesized by Qian's and Yu's groups, respectively.[19,20] To the best of our knowledge, however, the synthesis of NaV_6O_{15} and $Na_2V_6O_{16}\cdot 3H_2O$ (barnesite) nanowires has never been reported. Here, we describe a facile hydrothermal method to selectively grow NaV_6O_{15} and $Na_2V_6O_{16}\cdot 3H_2O$ nanowires from simple initial materials of V_2O_5, $NaHSO_4\cdot H_2O$, and Na_2SO_4 without the use of catalysts or templates.

Experimental Section

All starting materials were of analytic reagent grade, and deionized water was used as solvent. Vanadium pentaoxide powder was purchased from BDH Chemicals Ltd. $NaHSO_4\cdot H_2O$ and Na_2SO_4 were from ACROS. All chemicals were used directly without further treatment. In a typical synthesis of NaV_6O_{15} nanowires, 0.5 mmol of V_2O_5 powders and 1.0 mmol

* Corresponding author: Dr. Gen-Tao Zhou, E-mail: gtzhou@ustc.edu.cn.
† University of Science and Technology of China.
‡ The Chinese University of Hong Kong.

10.1021/cg0496686 CCC: $30.25
Published on Web 12/15/2004

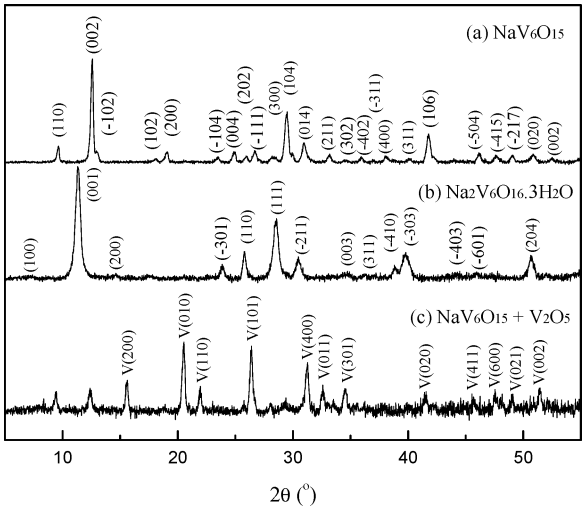

Figure 1. Typical XRD patterns of NaV_6O_{15} (a), $Na_2V_6O_{16}\cdot 3H_2O$ (b) nanowires, and a mixture of NaV_6O_{15} and V_2O_5 (c).

of $NaHSO_4\cdot H_2O$ were loaded into a 20 mL capacity Teflon-lined stainless steel autoclave, and then 15 mL of deionized water was added into the Teflon-lined stainless steel autoclave. The autoclave containing the reactant solution was sealed and placed into a programmed furnace to be kept at 180 °C for 24 h, and then it was naturally cooled to room temperature. The resulting precipitate was collected and washed with deionized water and absolute ethanol to remove ions possibly remaining in the final product, and finally dried at 60 °C overnight in a vacuum oven. Similar procedures were adopted for the $Na_2V_6O_{16}\cdot 3H_2O$ nanowires. A total of 1.0 mmol of anhydrous Na_2SO_4 instead of $NaHSO_4\cdot H_2O$ was used. Moreover, the initial and final pH values of the solutions were measured to be ca. 2.0 and 1.8 for NaV_6O_{15} nanowires, and 5.5 and 2.2 for $Na_2V_6O_{16}\cdot 3H_2O$, respectively.

Several analytical techniques were used to characterize the synthesized products. X-ray powder diffraction patterns were recorded on a Bruker D8 Advance Power X-ray diffractometer (using Cu Kα $\lambda = 0.15418$ nm radiation) operating at 40 kV/40 mA, with a graphite reflected beam monochromator and variable divergence slits. The scanning rate was 0.02°/s. The morphology and size of as-prepared particles were examined by a LEO 1450VP scanning microscope operating at 20 kV. TEM photographs, SAED patterns, and EDX analyses were recorded on a JEOL JEM-2010F field emission transmission electron microscope at an acceleration voltage of 200 kV. The X-ray photoelectron spectra (XPS) were collected on an ESCALab MKII X-ray photoelectron spectrometer, using non-monochromatized Mg Kα X-ray as the excitation source. Thermogravimetric analysis was conducted on a SHIMADZU TGA-50 thermogravimetric analyzer under the flowing air atmosphere.

Results and Discussion

The purity and crystallinity of the as-prepared product were determined using powder XRD. Figure 1a,b shows the typical XRD patterns of the synthesized products. Combining JCPDS file no. 49-0998 with the data in the literature,[17b] Figure 1a can be indexed as monoclinic NaV_6O_{15} with lattice parameters of $a = 10.10$ Å, $b = 3.63$ Å, and $c = 15.45$ Å, $\beta = 110°$. Compared with JCPDS file no. 16-0601, all of the reflections in Figure 1b could be indexed as the monoclinic $Na_2V_6O_{16}\cdot 3H_2O$ with lattice parameters of $a = 12.17$ Å, $b = 3.602$ Å, and $c = 7.78$ Å, $\beta = 95.03°$. These results are consistent with those of NaV_6O_{15} and $Na_2V_6O_{16}\cdot 3H_2O$ bulk crystals. XRD patterns indicate that pure phase of NaV_6O_{15} or $Na_2V_6O_{16}\cdot 3H_2O$ nanowires derived from our current synthetic method can readily be obtained.

The size and morphology of the products were examined by scanning electron microscopy. Low magnification SEM observations to the products of NaV_6O_{15} and $Na_2V_6O_{16}\cdot 3H_2O$ (Figure 2A,B) exhibit large-scale wire-like morphology, and there are no traces of nanorods and nanoparticles. The nanowires of NaV_6O_{15} existing in the form of single wires or some wire bundles are straight and have uniform and smooth diameters along the growth direction. To the best of our knowledge, this is the first report of the synthesis of a 1D nanostructure of NaV_6O_{15}. Compared with the nanowires of NaV_6O_{15}, the $Na_2V_6O_{16}\cdot 3H_2O$ product consists of curved, thinner wire-like structures. Furthermore, high magnification SEM analyses confirmed the synthesized products are composed of nanowire morphology, as shown in Figure 2C,D. NaV_6O_{15} nanowires have an average diameter of 80 nm and several tens of micrometers in length, while $Na_2V_6O_{16}\cdot 3H_2O$ nanowires have a mean diameter of 60 nm and length up to 10 μm.

TEM and HRTEM observations for individual nanowires provide additional insight into the structure of these materials. The TEM images (Figure 3A,C) of representative single nanowires of NaV_6O_{15} and $Na_2V_6O_{16}\cdot 3H_2O$ further demonstrate that the obtained products have a uniform wire-like morphology. Selected area electron diffraction (SAED) analyses of NaV_6O_{15} and $Na_2V_6O_{16}\cdot 3H_2O$ taken from different parts of a single nanowire gave similar monoclinic ED patterns, revealing the single crystalline nature of the nanowires. The typical SAED patterns of NaV_6O_{15} and $Na_2V_6O_{16}\cdot 3H_2O$ are shown in insets of Figure 3, panels A and C, respectively. The HRTEM images B and D taken from the single nanowires (Figure 3A,C) show the clearly resolved lattice fringes, corresponding to the $(\bar{1}04)$ and (001) planes of NaV_6O_{15} and $Na_2V_6O_{16}\cdot 3H_2O$, respectively. The $(\bar{1}04)$ planes in NaV_6O_{15} and the (001) planes in $Na_2V_6O_{16}\cdot 3H_2O$ are oriented parallel to respective nanowire growth direction. These substantiate that the nanowires are single crystalline. EDX analyses (see Supporting Information) from different positions along the nanowires show the chemical signatures of the nanowires are identical within experimental error and that these nanowires are composed of Na, V, and O elements, indicating that the analyzed nanowires are our target products, i.e., NaV_6O_{15} and $Na_2V_6O_{16}\cdot 3H_2O$.

XPS analyses further confirm the structures of NaV_6O_{15} and $Na_2V_6O_{16}\cdot 3H_2O$ nanowires. As shown in Figure 4, the survey spectra demonstrate the presence of the elements of Na, V, and O. The high-resolution XPS spectra from V 2p to O 1s region of the nanowires of NaV_6O_{15} and $Na_2V_6O_{16}\cdot 3H_2O$ show that the binding energies (BE) of V $2p_{3/2}$ (516.35 eV), V $2p_{1/2}$ (523.71 eV) and O1s (529.15 eV) in $Na_2V_6O_{16}\cdot 3H_2O$ nanowires shift toward the smaller binding energy relative to those in NaV_6O_{15} nanowires [V $2p_{3/2}$ (517.05 eV), V $2p_{1/2}$ (524.51 eV) and O 1s (529.75 eV)], indicating the chemical bonds of vanadium and oxygen in NaV_6O_{15} differ from similar

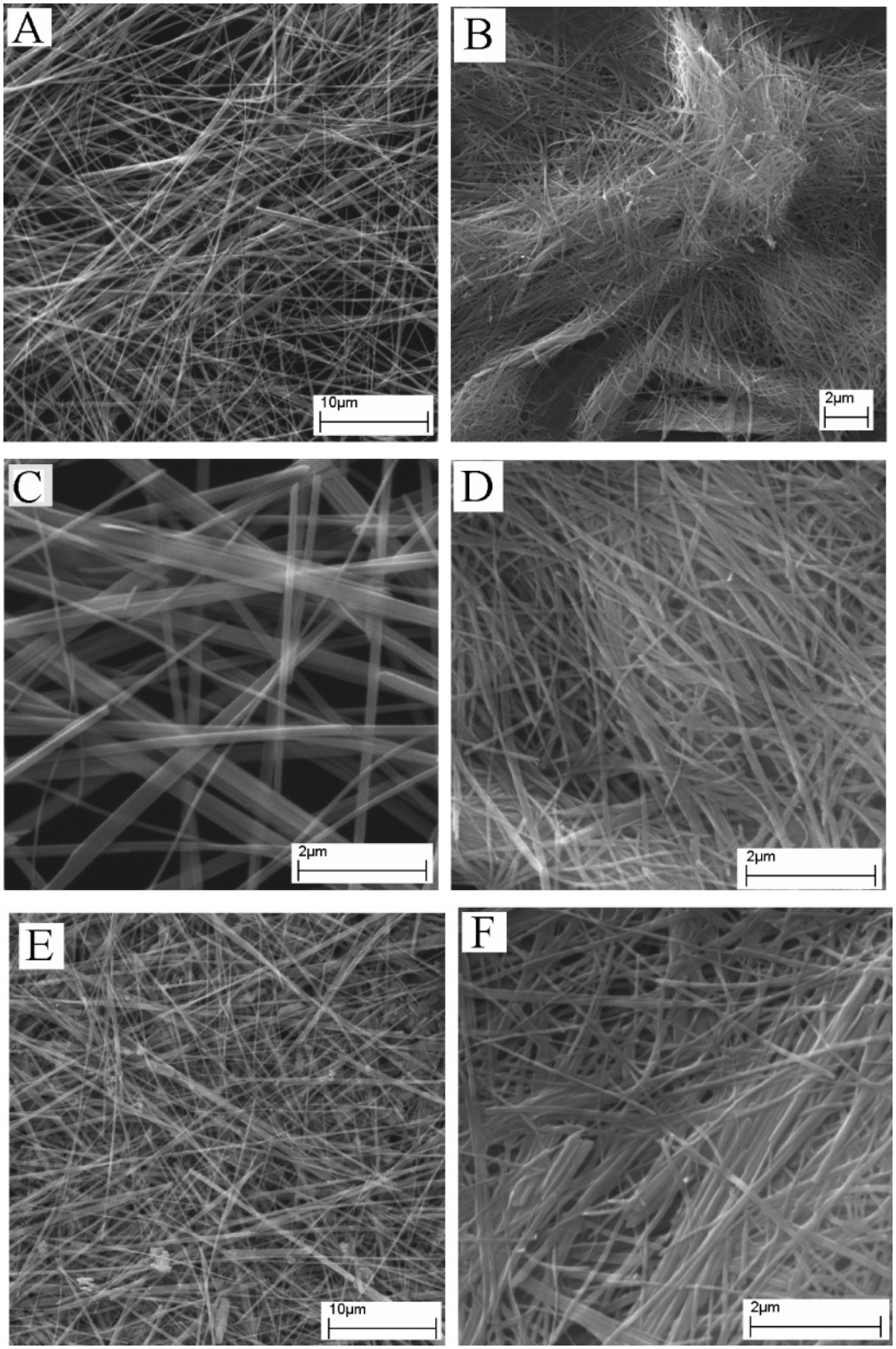

Figure 2. Representative SEM images of NaV_6O_{15} (A, C), $Na_2V_6O_{16}\cdot 3H_2O$ (B, D) nanowires, a mixture of NaV_6O_{15} and V_2O_5 (E) and $Na_2V_6O_{16}\cdot 3H_2O$ (F) nanowires prepared at 140 °C.

bonds in $Na_2V_6O_{16}\cdot 3H_2O$. The lower intensity O1s peak centered near 531.71 eV in $Na_2V_6O_{16}\cdot 3H_2O$ can be attributed to the O−H bond of H_2O. Additional supporting information was obtained by thermogrivimetric ananlysis (see Supporting Information), which gave a weight loss of 7.6%, close to the theoretical dehydration percentage of 8.2%. The high-resolution spectrum of NaV_6O_{15} also shows that V $2p_{3/2}$ consists of two overlapping peaks. The peak at BE = 517.05 eV may be assigned to V^{5+} ions, and the one at BE = 515.42 eV to V^{4+} ions. Such overlapping peaks are usually observed in ternary vanadium oxide bronzes containing mixed valences of V^{5+} and V^{4+}.[21] So, the XPS analyses testify that two different kinds of nanowires of sodium vanadium oxides were synthesized.

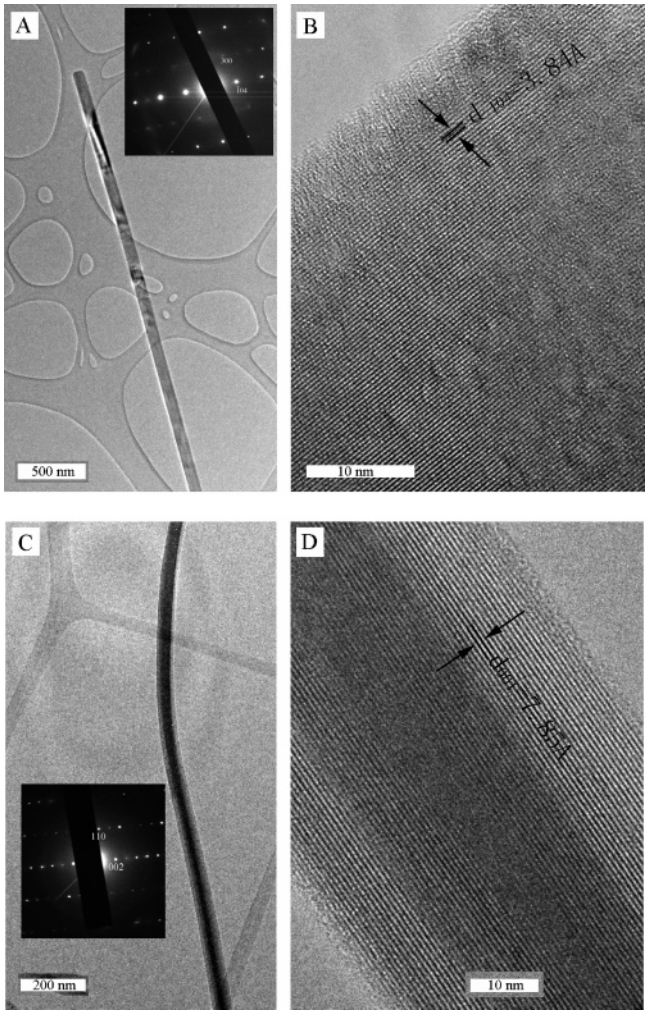

Figure 3. TEM and HRTEM images of single nanowires of NaV_6O_{15} (A, B) and $Na_2V_6O_{16}\cdot 3H_2O$ (C, D).

Under the present hydrothermal conditions, the formation of nanowires can be described by the following reactions:

$$2NaHSO_4 + 6V_2O_5 + H_2O \rightarrow 2NaV_6O_{15} + H_2SO_3 + O_2 + H_2SO_4 \quad (1)$$

$$2Na_2SO_4 + 3V_2O_5 + 4H_2O \rightarrow Na_2V_6O_{16}\cdot 3H_2O + 2NaHSO_4 \quad (2)$$

Reaction 1 is a redox process associated with the following two half reactions:

$$VO_2^+ + 2H^+ + e \rightarrow VO^{2+} + H_2O \ (E^0 = 1.0\ V)$$

$$O_2 + H_2SO_3 + 2e \rightarrow SO_4^{2-} + H_2O \ (E^0 = 1.0\ V)$$

The standard reduction potentials show that reaction 1 has a weak redox tendency. However, the hydrothermal treatment in the acidic environment[22] can provide a driving force for reaction 1 to proceed. It is the weak redox tendency that results in partial reduction of VO_2^+ to VO^{2+}, so that only NaV_6O_{15} nanowires but not $VOSO_4$ or other vanadium oxides could be formed. In contrast, the same concentration of Na_2SO_4 instead of $NaHSO_4$ was utilized, and as a result, metathetical reaction 2 led to $Na_2V_6O_{16}\cdot 3H_2O$ nanowires under the same hydrothermal conditions. In this regard, a selected-control synthesis for NaV_6O_{15} or $Na_2V_6O_{16}\cdot 3H_2O$ nanowires was achieved.

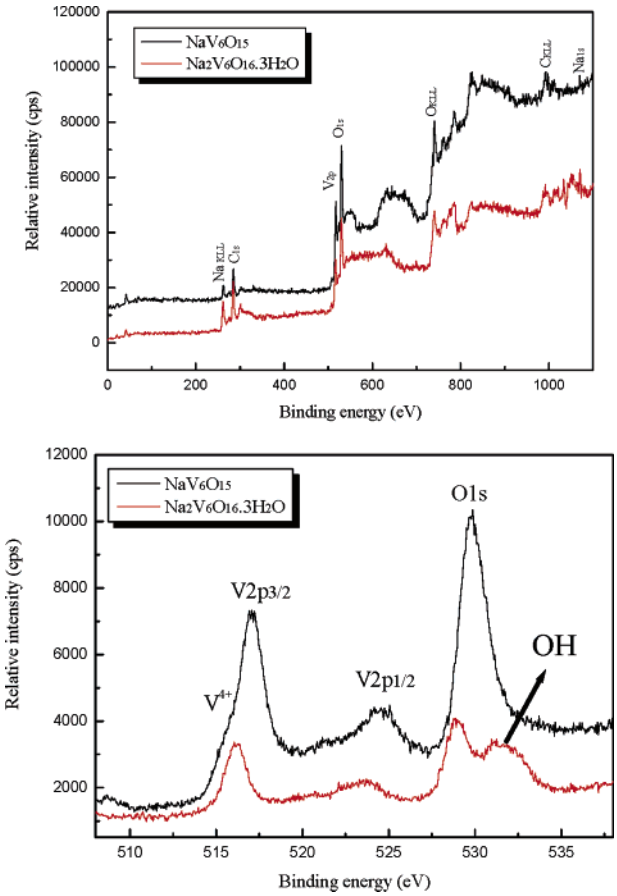

Figure 4. XPS spectra of the synthesized NaV_6O_{15} and $Na_2V_6O_{16}\cdot 3H_2O$ nanowires.

Moreover, our experiments also show that an excess amount of sulfate ($NaHSO_4\cdot H_2O$ or Na_2SO_4) and a sufficiently high reaction temperature are required for the formation of pure phase nanowires. When a stoichiometric amount of sulfate was used, no nanowires of NaV_6O_{15} or $Na_2V_6O_{16}\cdot 3H_2O$ could be obtained. So, the excess of sulfate ensures the formation of our target product under present experimental conditions. A series of different hydrothermal temperature experiments were carried out. A mixture of NaV_6O_{15} nanowires and V_2O_5 particles would be formed at a lower reaction temperature of 160 °C. This was confirmed by XRD and SEM analyses. The typical XRD pattern and SEM image are shown in Figure 1c and Figure 2E, respectively. Both XRD and SEM analyses indicate that V_2O_5 and NaV_6O_{15} coexist. For the V_2O_5–Na_2SO_4–H_2O hydrothermal system, when hydrothermal temperatures ranged from 180 to 140 °C, pure nanowires of $Na_2V_6O_{16}\cdot 3H_2O$ can be obtained. A representative SEM image of $Na_2V_6O_{16}\cdot 3H_2O$ nanowires synthesized at 140 °C is also presented in Figure 2F. Compared with the SEM image D of the sample synthesized at 180 °C, negligible differences in morphology and size can be found. This means that a facile hydrothermal process leads to the formation of nanowires.

Although the exact mechanism for the formation of these uniform nanowires is still unclear, we believe that

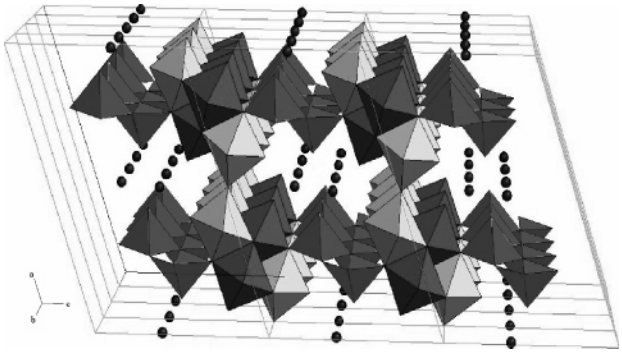

Figure 5. Schematic diagram of the NaV_6O_{15} crystal structure.

the growth of the nanowires is controlled by a solid−solution−solid process (SSS). Vanadium pentoxide is first dissolved and hydrolyzed under hydrothermal conditions to form various species such as VO_2^+, VO_3^-, VO_4^{3-}, and $H_2VO_4^-$. In a neutral-to-acidic reaction system, these species condense and polymerize to polyvanadates chains,[23] further linking up through sharing the edges or the corners to form 3D frameworks structure. The sodium ions can accommodate these framework tunnels. As a result, the preferential growth nanowires are formed. This proposed mechanism is consistent with the vanadate sodium crystal structure. Figure 5 is a crystal structure schematic diagram of NaV_6O_{15} ($Na_{0.33}V_2O_5$). It clearly shows the double chains of octahedral that can be linked up through corners in the *c* axis direction and also in the *a* direction by chains of V atoms in 5-coordination.[24] Such a chain structure may contribute to the 1D growth.

The shape of a nanocrystal can be determined by the relative specific surface energies associated with the facets of the crystal.[25] Moreover, control of size and shape are also attributed to the presence of the directing agent, which functions as a hard or soft template (such as porous alumina membranes or micelles). It is now widely believed that preferential absorption of molecules and ions in solution to different crystal faces directs the growth of nanoparticles into various shapes by controlling the growth rates along different crystal axes.[13c,26] Here, it is the preferential adsorption of SO_4^{2-} in solution to different crystal faces that directs the growth of nanoparticles to their ultimate nanowire morphology. This is confirmed by our control experiments. The controlled experiments using NaCl instead of Na_2SO_4 showed that no nanowires could be formed, indicating that SO_4^{2-} plays a crucial role in nanowire formation. Furthermore, Yu et al. also reported that in the presence of F^- anions nanobelts of $Na_2V_6O_{16}\cdot 3H_2O$ were obtained, with widths of 60 to 500 nm.[20] This further supports that the SO_4^{2-} anions are crucial for the growth of the nanowires. It is well-known that SO_4^{2-} has a stronger coordination ability than halogen anions. It appears that selected adsorption of SO_4^{2-} anions to the special crystal facets may result in the formation of 1D nanowires, rather than nanobelts.

Conclusion

In summary, a novel and simple hydrothermal approach has been successfully developed to prepare NaV_6O_{15} and $Na_2V_6O_{16}\cdot 3H_2O$ nanowires. SAED and HRTEM analyses confirm that the nanowires are single crystalline. The key factors to control the morphology and a possible formation mechanism were discussed. The new synthetic route is also expected to be applicable to the synthesis of other metal vanadium oxide nanowires.

Acknowledgment. The work described in this paper was partially supported from the Natural Science Foundation of China (Project Nos. 49903001) and the Research Grants Council of the Hong Kong Special Administrative Region, China. (Project No. CUHK 4027/02P). We thank Prof. Ji Ming-Rong for his assistance with XPS measurements.

Supporting Information Available: EDX spectra of NaV_6O_{15} and $Na_2V_6O_{16}\cdot 3H_2O$ nanowires (Figure S1) and thermogravimetric analysis of the synthesized $Na_2V_6O_{16}\cdot 3H_2O$ nanowires (Figure S2). This material is available free of charge via the Internet at http://pubs.acs.org.

References

(1) (a) Huang, M. H.; Maom, S.; Feick, H.; Yan, H. Q.; Wu, Y. Y.; Kind, H.; Weber, E.; Russo, R.; Yang, P. D. *Science* **2001**, *292*, 1897. (b) Duan, X.; Huang, Y.; Agarwal, R.; Lieber, C. M. *Nature* **2003**, *421*, 241. (c) Zhang, R. Q.; Lifshitz, Y.; Lee, S. T. *Adv. Mater*. **2003**, *15*, 635. (d) Ye, C. H.; Meng, G. W.; Jiang, Z.; Wang, Y. H.; Wang, G. Z.; Zhang, L. D. *J. Am. Chem. Soc.* **2002**, *124*, 15180. (e) Duan, X.; Lieber, C. M. *Adv. Mater*. **2000**, *12*, 298. (f) Pan, Z. W.; Dai, Z. R.; Wang, Z. L. *Science* **2001**, *291*, 1947. (g) Sun, Y. G.; Gates, B.; Mayers, B.; Xia, Y. N. *Nano Lett*. **2002**, *2*, 165. (h) Jiang, Y.; Meng, X. M.; Liu, J.; Hong, Z. R.; Lee, C. S.; Lee, S. T. *Adv. Mater.* **2003**, *15*, 1195. (i) Wang, Y. L.; Jian, X. C.; Xia, Y. N. *J. Am. Chem. Soc*. **2003**, *125*, 16176. (j) Nath, M.; Choudhury, A.; Kundu, A.; Rao, C. N. R. *Adv. Mater.* **2003**, *15*, 2098.

(2) (a) Chung, S. W.; Yu, J. Y.; Heath, J. R. *Appl. Phys. Lett.* **2000**, *76*, 2068. (b) Tans, J. S.; Verschueren, R. M.; Dekker, C. *Nature* **1998**, *393*, 49.

(3) Duan, X.; Huang, Y.; Cui, Y.; Wang, J.; Lieber, C. M. *Nature* **2001**, *409*, 66.

(4) (a) Tans, S. J.; Devoret, M. H.; Dal, H.; Thess, A.; Smalley, R. E.; Gerrligs, L. J.; Dekker, C. *Nature* **1997**, *386*, 474. (b) Bockrath, M.; Cobden, D. H.; McEuen, P. L.; Chopra, N. G.; Zettl, A.; Thess, A.; Smalley, R. E. *Science* **1997**, *275*, 1922.

(5) (a) Cui, Y.; Wei, Q.; Park, H.; Lieber, C. M. *Science* **2001**, *293*, 1289. (b) Nicewarner-Peña, S. R.; Freeman, R. G.; Reiss, B. D.; He, L.; Peña, D. J.; Walton, I. D.; Cromer, R.; Keating, C. D.; Natan, M. J. *Science* **2001**, *294*, 137.

(6) Wang, J.; Gudiksen, M. S.; Duan, X.; Cui, Y.; Lieber, C. M. *Science* **2001**, *293*, 1455.

(7) Davydov, D. N.; Sattari, P. A.; AlMawlawi, D.; Osika, A.; Haslett, T. L.; Moskovits, M. *J. Appl. Phys.* **1999**, *86*, 3983.

(8) Yan, H.; He, R.; Johnson, J.; Law, M.; Saykally, R.; Yang, P. D. *J. Am. Chem. Soc.* **2003**, *125*, 4728.

(9) (a) Hu, J.; Odom, T. W.; Lieber, C. M. *Acc. Chem. Res*. **1999**, *32*, 435. (b) Morales, A. M.; Lieber, C. M. *Science* **1998**, *279*, 208. (c) Gudiksen, M. S.; Lieber, C. M. *J. Am. Chem. Soc*. **2000**, *122*, 8801. (d) Cui, Y.; Lauhon, L. J.; Gudiksen, M. S.; Wang, J. F.; Lieber, C. M. *J. Phys. Lett.* **2001**, *78*, 2214. (e) Barrelet, C. J.; Wu, Y.; Bell, D. C.; Lieber, C. M. *J. Am. Chem. Soc.* **2003**, *125*, 11498.

(10) Trentler, T. J.; Hickman, K. M.; Goel, S. C.; Viano, A. M.; Gibbons, P. C.; Buhro, W. E. *Science* **1995**, *270*, 1791.

(11) (a) Lee, S. T.; Wang, N.; Zhang, Y. F.; Tang, Y. H. *MRS Bull.* **1999**, 36. (b) Wang, N.; Tang, Y. H.; Zhang, Y. F.; Lee, C. S.; Lee, S. T. *Phys. Rev. B* **1998**, *58*, R16024.

(12) Ge, J. P.; Li, Y. D. *Chem. Commun*. **2003**, 2498.

(13) (a) Wu, Y. Y.; Yan, H.; Huang, M. Q.; Messer, B.; Song, J. H.; Yang, P. D. *Chem. Eur. J.* **2002**, *8*, 1260. (b) Song, J. H.; Messer, B.; Wu, Y. Y.; Kind, H.; Yang, P. D. *J. Am. Chem. Soc.* **2001**, *123*, 9714. (c) Puntes, V. F.; Krishnan, K. M.;

Alivisatos, A. P. *Science* **2001**, *291*, 2115. (d) Mbindyo, J. K. N.; Mallouk, T. E.; Mattzela, J. B.; Kratochvilova, I.; Razavi, B.; Jackson, T. N.; Mayer, T. S. *J. Am. Chem. Soc.* **2002**, *124*, 4020. (e) Cao, M. H.; Hu, C. W.; Peng, G.; Qi, Y. J.; Wang, E. B. *J. Am. Chem. Soc*. **2003**, 4982. (f) Lee, S. M.; Cho, S. N.; Cheon, J. *Adv. Mater*. **2003**, *15*, 441.

(14) Rao, C. N. R.; Deepak, F. L.; Gundiah, G.; Govindaraj, A. *Prog. Solid State Chem.* **2003**, *31*, 5.

(15) Xia, Y. N.; Yang, P. D.; Yu, Y. G.; Wu, Y. Y.; Mayers, B.; Gates, B.; Yin, Y. D.; Kim, F.; Yan, H. Q. *Adv. Mater.* **2003**, *15*, 353.

(16) (a) Fang, Y. P.; Xu, A. W.; Song, R. Q.; Zhang, H. X.; You, L. P.; Yu, J. C.; Liu, H. Q. *J. Am. Chem. Soc.* **2003**, *125*, 16025. (b) Patzke, G. R.; Krumeich, F.; Nesper, R. *Angew. Chem., Int. Ed.* **2002**, *41*, 2446. (c) Vayssieres, L. *Adv. Mater.* **2003**, *15*, 464. (d) Wang, X.; Li, Y. D. *J. Am. Chem. Soc*. **2002**, *124*, 2880. (e) Holmes, J. D.; Johnston, K. P.; Doty, R. C.; Korgel, B. A. *Science* **2000**, *287*, 1471. (f) Niederberger, M.; Muhr, H. J.; Krumeich, F.; Bieri, F.; Günther, D.; Nesper, R. *Chem. Mater*. **2000**, *12*, 1995.

(17) (a) Livage, J. *Coord. Chem. Rev.* **1999**, *391*, 190. (b) Millet, M.; Pereira-Ramos, J. P.; Sabbar, E. M.; De Roy, M. E.; Besse, J. P. *Solid State Ionics* **1998**, *112*, 319. (c) Livage, J.; Ganguli, D. *Solar Energy Mater. Solar Cells* **2001**, 365. (d) Gregoire, G.; Souban, P.; Farcy, J.; Pereira-Ramos, J. P.; Badot, J. C.; Baffier, N. *J. Power Sources* **1999**, *81*−*82*, 612. (e) Inubushi, A.; Masuda, S.; Okuto, M.; Matsumoto, A.; Sadamura, H.; Suzuki, K. In *High Technology Ceramics*; Vincenzini, P., Ed.; Elsevier: Amsterdam, 1987, p 2165.

(18) (a) Itoh, M.; Akimoto, N.; Yamada, H.; Isobe, M.; Ueda, Y. *Physics C* **2000**, *341*−*348*, 2133. (b) Vasil'ev, A. N.; Marchenko, V. I.; Smirnov, A. I.; Sosin, S. S.; Yamada, H.; Ueda, Y. *Phys. Rev. B* **2001**, *64*, 174403.

(19) Kong, L. F.; Shao, M. W.; Xie, Q.; Liu, J. W.; Qian, Y. T. *J. Cryst. Growth* **2004**, *260*, 435.

(20) Yu, J. G.; Yu, J. C.; Ho, W. K.; Wu, L.; Wang, X. C. *J. Am. Chem. Soc*. **2004**, *126*, 3422.

(21) Rozier, P.; Galy, J.; Chelkowska, G.; Koo, H.-J.; Whangbo, M.-H. J. *Solid State Chem.* **2002**, *166*, 382.

(22) Cotton, F. A.; G. Wilkinson F. R. S. *Advances in Inorganic Chemistry*, 3rd ed.; John Wiley & Sons: New York, 1972; p 821.

(23) Pope, M. T.; Dale, B. W. *Quart. Rev.* **1968**, *22*, 527.

(24) Wells, A. F. *Structural Inorganic Chemistry*, 3rd ed.; Clarendon Press: Oxford, 1962, p 689.

(25) (a) Mao, Y.; Banerjee, S.; Wong, S. S. *J. Am. Chem. Soc*. **2003**, *125*, 15718. (b) Blagden, N. In *Crystal Engineering: The Design Application of Functional Solids*; Seddon, K. R., Zaworotko, M., Eds.; Kluwer Academic Publishers: Dordrecht, 1999; pp 127−153.

(26) (a) Murphy, C. J. *Science* **2002**, *298*, 2139. (b) Sun, Y. G.; Xia, Y. N. *Science* **2002**, *298*, 2176. (c) Filankembo, A.; Giorgio, S.; Lisiecki, I.; Pileni, M. P. *J. Phys. Chem. B* **2003**, *107*, 7492.

CG0496686